Structurally novel PI3Kδ/γ dual inhibitors characterized by a seven-membered spirocyclic spacer: The SARs investigation and PK evaluation

Qiangqiang Tao, Yuqing Chen, Xiao Liang, Yongzhou Hu, Jiaming Li, Fang Fang, Huchuan Wang, Chang Meng, Jingtai Liang, Xiaodong Ma, Shuangying Gui

PII: S0223-5234(20)30110-0

DOI: https://doi.org/10.1016/j.ejmech.2020.112143

Reference: EJMECH 112143

To appear in: *European Journal of Medicinal Chemistry*

Received Date: 2 December 2019

Revised Date: 29 December 2019

Accepted Date: 11 February 2020

Please cite this article as: Q. Tao, Y. Chen, X. Liang, Y. Hu, J. Li, F. Fang, H. Wang, C. Meng, J. Liang, X. Ma, S. Gui, Structurally novel PI3Kδ/γ dual inhibitors characterized by a seven-membered spirocyclic spacer: The SARs investigation and PK evaluation, *European Journal of Medicinal Chemistry* (2020), doi: https://doi.org/10.1016/j.ejmech.2020.112143.

Graphical abstract

Structurally novel PI3Kδ/γ dual inhibitors characterized by a seven-membered spirocyclic spacer: the SARs investigation and PK evaluation

Qiangqiang Tao [a], Yuqing Chen [a], Xiao Liang [a], Yongzhou Hu [d], Jiaming Li [a, b], Fang Fang [a, b], Huchuan Wang [a, b], Chang Meng [a], Jingtai Liang [a], Xiaodong Ma [a, b, *], Shuangying Gui [a, c, *]

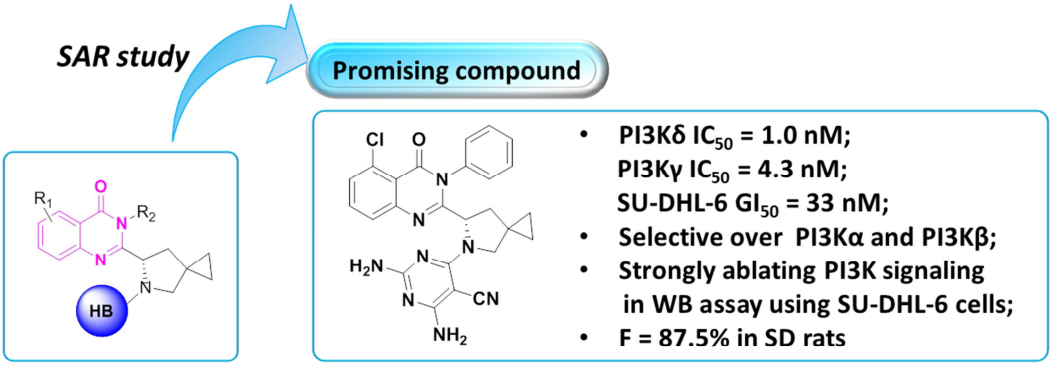

Structurally novel PI3Kδ/γ dual inhibitors characterized by a seven-membered spirocyclic spacer: the SARs investigation and PK evaluation

Qiangqiang Tao [a], Yuqing Chen [a], Xiao Liang [a], Yongzhou Hu [d], Jiaming Li [a, b], Fang Fang [a, b], Huchuan Wang [a, b], Chang Meng [a], Jingtai Liang [a], Xiaodong Ma [a, b, *], Shuangying Gui [a, c, *]

a. College of Pharmacy, Anhui University of Chinese Medicine, Hefei 230012, China

b. Institute of Medicinal Chemistry, Anhui Academy of Chinese Medicine, Hefei 230012, China

c. Institute of Pharmaceutics, Anhui Academy of Chinese Medicine, Hefei 230012, China

d. ZJU-ENS Joint Laboratory of Medicinal Chemistry, Zhejiang Province Key Laboratory of Anti-Cancer Drug Research, College of Pharmaceutical Sciences, Zhejiang University, Hangzhou 310058, China

Abstract: Herein, we communicate our recent medicinal chemistry efforts which have culminated in a series of PI3Kδ/γ dual inhibitors structurally featuring a seven-membered spirocyclic spacer. Compound **26**, the most potent one among them, exhibited superior PI3Kδ inhibitory activity (IC_{50} = 1.0 nM) to that of the approved PI3Kδ inhibitor Idelalisib. Besides, it exerted remarkable anti-proliferative efficacy against human malignant B-cell line SU-DHL-6 with GI_{50} value of 33 nM. The biochemical assay against the other three class I PI3K isoforms identified compound **26** as a potent PI3Kδ/γ dual inhibitor with considerable selectivity over PI3Kα and PI3Kβ. In SU-DHL-6 cells, a dramatic down-regulation of PI3K signaling was observed following compound **26**-treatment at the concentration as low as 10 nM. Inspiringly, the pharmacokinetic (PK) study in Sprague-Dawley (SD) rats revealed it was orally available with a favorable bioavailability (F = 87.5%). Overall, compound **26**, a promising PI3Kδ/γ dual inhibitor, has the potential to emerge as a clinical candidate for the treatment of leukocyte-mediated malignancies after extensive functional investigation.

Key words: Spirocyclic spacer; PI3Kδ/γ dual inhibitor; Anti-proliferative efficacy; PI3K signaling; PK study

* Corresponding author: Xiaodong Ma

College of Pharmacy, Anhui University of Chinese Medicine, Hefei 230012, China;

Institute of Medicinal Chemistry, Anhui Academy of Chinese Medicine, Hefei 230012, China

E-mail: o-omaxiaodong@163.com

* Corresponding author: Shuangying Gui

College of Pharmacy, Anhui University of Chinese Medicine, Hefei 230012, China;

Institute of Pharmaceutics, Anhui Academy of Chinese Medicine, Hefei 230012, China

E-mail: guishy0520@126.com

1. Introduction

The preferential distribution of phosphoinositide 3-kinase δ (PI3Kδ) in leukocytes offers a unique opportunity for pharmacologically interfering with this isoform in the treatment of leukocyte-mediated conditions driven by its pathologic activation [1, 2]. Besides the vital role in triggering the proliferation, survival and trafficking of malignant B-cell [3], PI3Kδ, located downstream of receptor tyrosine kinases (RTKs) [4], has been proven hyperactive in autoimmune, inflammatory and allergic disorders, including rheumatoid arthritis (RA), allergic asthma, psoriasis, and systemic lupus erythematosus (SLE) [5-8]. The approval of Idelalisib (Zydelig, **1**, **Fig. 1**) in 2014 is a testimony to the merit of PI3Kδ selective inhibitors as therapeutics for relapsed/refractory B-cell malignancies [9, 10]. Additionally, in the oncology setting, Umbralisib (TGR1202, **2**), Dezapelisib (INCB040093, **3**), Parsaclisib (INCB050465, **4**) and ME401 **5** have been progressed into clinical trials (**Fig. 1**) [11-13]. Meanwhile, Seletalisib (UCB5857, **6**) [14], Leniolisib (CDZ173, **7**) [15], Nemiralisib (GSK2269557, **8**) [16, 17] and GSK2292767 **9** [16] are presently under clinical investigation as remedies for non-oncology diseases, exemplified by respiratory, inflammatory and autoimmune conditions, as well as immunodeficiency (**Fig. 1**).

PI3Kγ, another class I PI3K subtype with restricted expression in leukocytes, is generally coupled to G protein-coupled receptors (GPCRs) rather than functioning downstream of RTKs [18]. However, apart from their complementary roles in inflammation and immune response [13], PI3Kγ and PI3Kδ concurrently mediate the proliferative and survival signaling in certain malignant hematopoietic cells [13, 19]. In particular, mounting evidences support their participation in modulating tumor microenvironment [20-23]. For instance, PI3Kγ can serve as a molecular switch that controls immune suppression via hampering phagocytosis by tumor-associated macrophages (TAMs), which negatively regulate effector T and natural killer (NK) cells in this state by expressing membrane-bound immune checkpoint molecules and secreting soluble immunosuppressive factors. Hence, concomitant inhibition of PI3Kδ and PI3Kγ has the potential to broaden the spectrum of anti-proliferative activity and achieve therapeutic synergism in hematologic malignancies, as well as inflammatory and autoimmune diseases [19, 24]. Duvelisib (Copiktra, **10**, **Fig. 1**) [25], marketed in 2018 for the treatment of B-cell mediated hematopoietic malignancies, is the first-in-class PI3Kδ/γ dual inhibitor. Tenalisib (RP6530, **11**) [26], also featuring PI3Kδ/γ bi-functional inhibitory activity, is currently clinically investigated in a combination therapy for classical Hodgkin's lymphomas (**Fig. 1**). Theoretically, owing to the

ubiquitous distribution of PI3Kα and PI3Kβ, both PI3Kδ-selective and PI3Kδ/γ dual inhibitors are beneficial to minimizing the off-target effects of pan-class I PI3Ks inhibitors in treating leukocyte-mediated conditions [27].

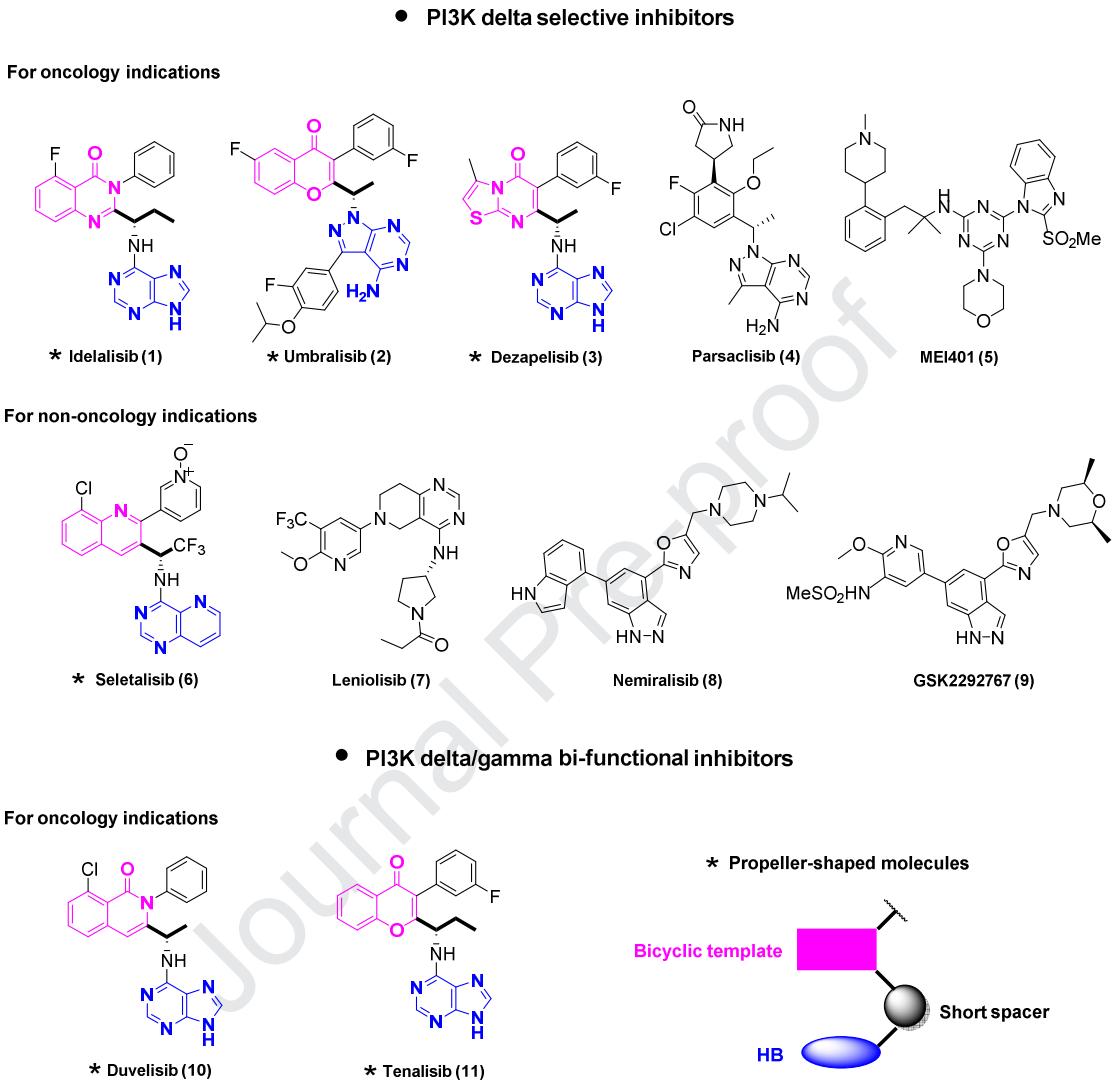

Fig. 1. Advanced PI3Kδ-selective or PI3Kδ/γ dual inhibitors: approved or under clinical trials

A considerable number of advanced PI3Kδ-selective and PI3Kδ/γ dual inhibitors are propeller-shaped molecules (**Fig. 1**), which share the same pharmacophore and simultaneously occupy the hinge region and the allosteric pocket of PI3Kδ catalytic cleft [13, 28, 29]. In respect of chemical structure, hinge binders (HBs) of them are routinely *N*-containing heteroaryl moiety tethered to a bicyclic heteroaryl template via a short spacer. While the HB is engaged in H-bond contacts with the enzyme, the bicyclic template inserts deeply into the allosteric hydrophobic pocket located between residues Trp760 and Met752 [30]. In contrast to the structurally diverse bicyclic templates, alteration in

the short spacer is relatively subtle among these propeller-shaped molecules. Spirocyclic building blocks are frequently employed in drug discovery for producing conformationally restricted molecules with structural novelty, and optimizing biological activity, pharmacokinetic (PK) property, as well as chemical stability [31-34]. During our recent medicinal chemistry campaign to broaden the structural diversity of the short spacer, a seven-membered spirocycle was introduced to replace the *S*-propylamine of **1**. We had speculated this structural elaboration, accompanied by modification at other sites, might affect the class I PI3K specificity profile of compounds. Built upon the resultant scaffold, structure-activity relationships (SARs) investigation on the replacement at the benzene ring of the bicyclic template (R_1), *N*-3 substituent (R_2) and HB was conducted to attain an optimum compound for further exploration (**Fig. 2**). As a consequence, compound **26** was discovered as a potent PI3Kδ/γ dual inhibitor with favorable *in vitro* performance and attractive PK profiles.

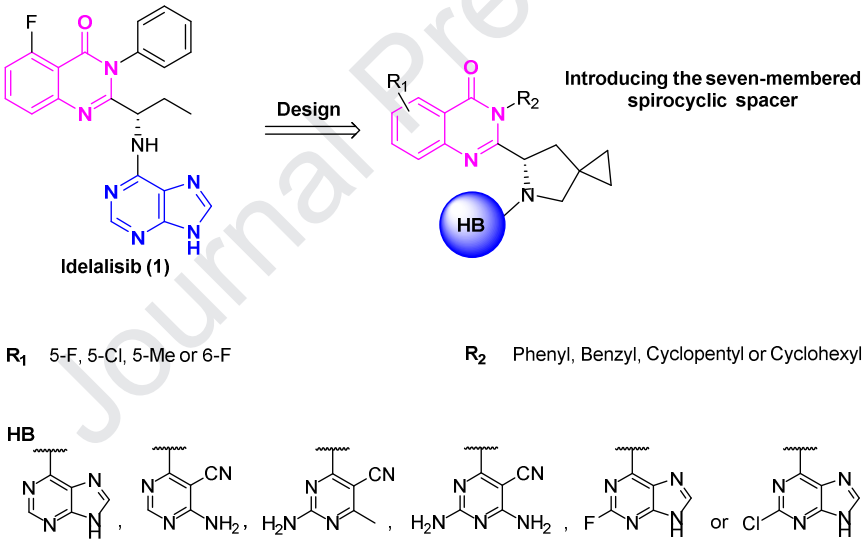

Fig. 2. The design rationale of target compounds and the focus of SARs study

2. Results and discussion

2.1. Chemistry

Compounds bearing phenyl as the *N*-3 substituent were synthesized according to **Scheme 1**. Condensation of ortho-amino benzoic acids **12a-d** with (*S*)-5-(*tert*-butoxycarbonyl)-5-azaspiro[2.4]heptane-6-carboxylic acid in the presence of $P(OPh)_3$, followed by the *in situ* treatment with aniline afforded the quinazolone derivatives **13a-d**. Afterwards,

removal of the Boc-protecting group and subsequent nucleophilic aromatic substitution (SNAr) reaction with 6-chloro-9*H*-purine, 4-amino-6-chloropyrimidine-5-carbonitrile, 2-amino-4-chloro-6-methylpyrimidine-5-carbonitrile, 6-chloro-2-fluoro-9*H*-purine or 2, 6-dichloro-9*H*-purine furnished **14-17**, **21**, **22**, **24**, **25** and **27-29** as target compounds. In addition, Boc-deprotected products of **13a** and **13b** were subjected to SNAr reaction with 2, 4-diamino-6-chloropyrimidine-5-carbonitrile in the presence of KF to generate compound **23** and **26**, respectively.

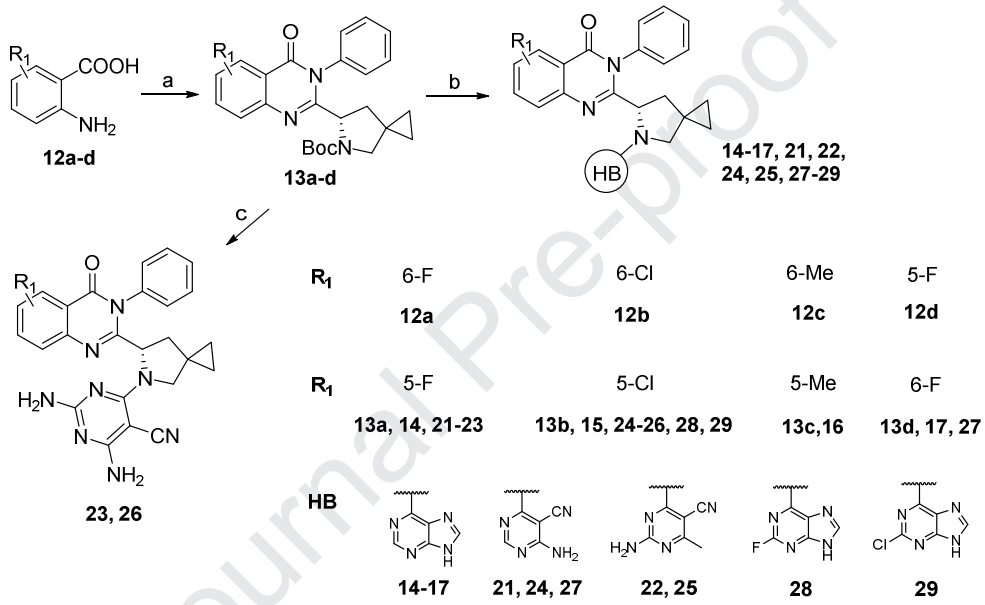

Scheme 1. Reagents and conditions:

(a) (1) (*S*)-5-(*tert*-butoxycarbonyl)-5-azaspiro[2.4]heptane-6-carboxylic acid, $P(OPh)_3$, pyridine, 70 °C, N_2; (2) aniline; (b) (1) trifluoroacetic acid (TFA)/dichloromethane (DCM), 0 °C to rt; (2) 6-chloro-9*H*-purine, 4-amino-6-chloropyrimidine-5-carbonitrile, 2-amino-4-chloro-6-methylpyrimidine-5-carbonitrile, 6-chloro-2-fluoro-9*H*-purine or 2, 6-dichloro-9*H*-purine, *N*, *N*-diisopropylethylamine (DIPEA), *t*-BuOH, 80 °C, N_2; (c) (1) TFA/DCM, 0 °C to rt; (2) 2, 4-diamino-6-chloropyrimidine-5-carbonitrile, KF, DIPEA, dimethyl sulfoxide (DMSO), 90 °C, N_2.

Scheme 2 displayed the synthetic route for compounds **18-20**. Amides **31a-c** were provided via conversion of 2-fluoro-6-nitrobenzoic acid **30** into the acyl chloride and the following condensation

with corresponding primary amine. Subsequently, **31a-c** were transformed into imidoyl chlorides, which underwent Mumm rearrangement after coping with (*S*)-5-(*tert*-butoxycarbonyl)-5-azaspiro[2.4]heptane-6-carboxylic acid to generate imides **32a–c**. After reduction of the nitro functionality, the *in situ* intra-molecular cyclization furnished quinazolone derivatives **33a-c**. Unmasking the nitrogen of the spirocycle and the ultimate SNAr reaction with 6-chloro-9*H*-purine afforded **18-20** as target compounds.

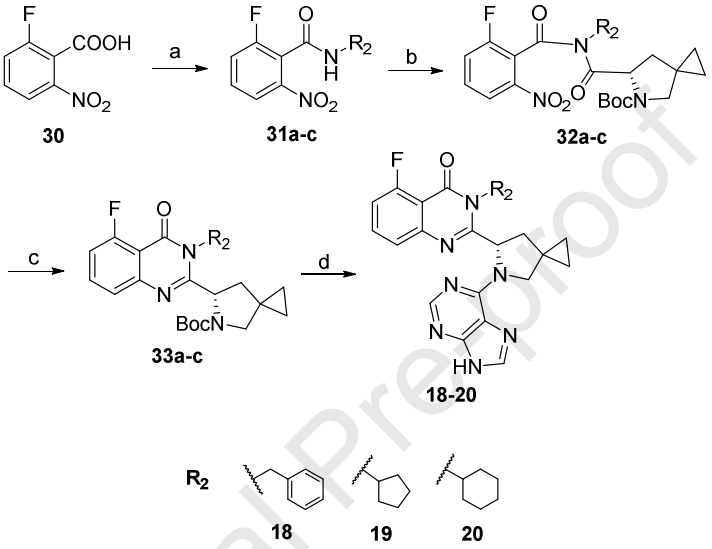

Scheme 2. Reagents and conditions: (a) (1) *N*, *N*-dimethylformamide (DMF), $SOCl_2$, 80 °C; (2) corresponding amine, anhydrous triethylamine (TEA), anhydrous DCM; (b) (1) DMF, $SOCl_2$, 80 °C, N_2; (2) (*S*)-5-(*tert*-butoxycarbonyl)-5-azaspiro[2.4]heptane-6-carboxylic acid, anhydrous TEA, anhydrous DCM, 0 °C to rt, N_2; (c) Zn, AcOH, 40 °C, N_2; (d) (1) TFA/DCM, 0 °C to rt; (2) 6-chloro-9*H*-purine, DIPEA, *t*-BuOH, 80 °C, N_2.

2.2. PI3Kδ biochemical assay

All the target compounds were firstly assayed against PI3Kδ for their inhibitory activity. According to the data presented in **Table 1**, a majority of them exerted remarkable PI3Kδ inhibitory activity with IC_{50} values below 50 nM, and six compounds exhibited IC_{50} values at single-digit nanomolar level. Among the target compounds, **26** displayed the most vigorous PI3Kδ inhibitory activity with IC_{50} value of 1.0 nM, which was more potent than that of Idelalisib.

Some valuable SARs were obtained from the enzymatic activity presented in **Table 1**. C-5 chloro replacement at the quinazolone template was more beneficial to PI3Kδ inhibitory potency than fluoro

replacement, as illustrated by the activity of **15** versus **14**, and **26** versus **23**. Alteration of C-5 fluoro substituent into C-6 fluoro substituent did not dramatically affect the activity (**17** versus **14**). With respect to the *N*-3 substituent, replacing the phenyl moiety with benzyl, cyclopentyl and cyclohexyl significantly weakened the enzymatic activity, as testified by the activity of **14** versus **18-20**. Among the various investigated HBs, it appeared evident that 2, 4-diaminopyrimidine-5-carbonitrile was optimum in accordance with the activity of **23** versus **14**, **21** and **22**, as well as **26** versus **15**, **24** and **25**. Besides, compounds with 4-aminopyrimidine-5-carbonitrile or 2-amino-6-methylpyrimidine-5-carbonitrile as HB were superior to corresponding compounds with purine as HB in PI3Kδ inhibitory potency (**21** and **22** versus **14**; **24** and **25** versus **15**). As for the purine moiety, the introduction of C-2 fluoro substituent slightly impaired the activity (**28** versus **15**), while the introduction of C-2 chloro substituent considerably lowered the enzymatic activity (**29** versus **15**).

Table 1. The PI3Kδ inhibitory activity of target compounds

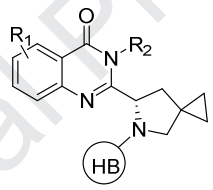

Cpd.	R_1	R_2	HB	PI3Kδ IC_{50} (nM)
14	5-F		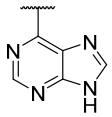	43
15	5-Cl		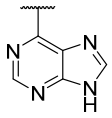	13
16	5-Me		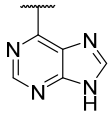	16
17	6-F		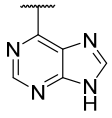	48
18	5-F	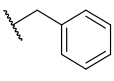	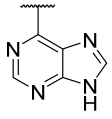	813
19	5-F		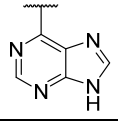	396

20	5-F		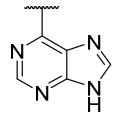	444
21	5-F		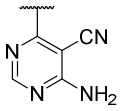	15
22	5-F		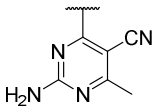	9.4
23	5-F		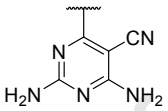	5.4
24	5-Cl		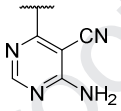	3.7
25	5-Cl		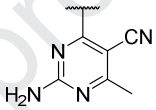	9.6
26	5-Cl		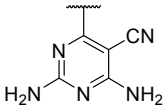	1.0
27	6-F		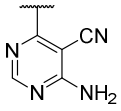	9.6
28	5-Cl		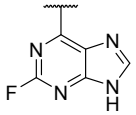	38
29	5-Cl		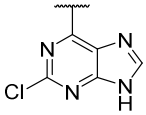	406
Idelalisib	---	---	---	3.4

2.3. Anti-proliferative assay

As stated in the introduction section, PI3Kδ signaling is critical for the proliferation of malignant B-cells. Hence, 3-(4, 5-dimethylthiazol-2-yl)-2, 5-diphenyltetrazolium bromide (MTT) assay was performed to evaluate the anti-proliferative activity of twelve compounds (PI3Kδ IC_{50}s < 50 nM) against human malignant B-cell line SU-DHL-6 and validate their potential for treating B-cell malignancies. On the whole, the anti-proliferative activity was consistent with the PI3Kδ inhibitory activity (**Table 2**). Compound **26**, with the most potent PI3Kδ inhibitory activity, also exerted the most remarkable anti-proliferative activity throughout this series against SU-DHL-6 cell line with GI_{50} value

of 33 nM. Besides, compound **23**, another one bearing 2, 4-diaminopyrimidine-5-carbonitrile as HB, displayed remarkable anti-proliferative activity against SU-DHL-6 cell line with GI_{50} value of 53 nM. Although replacement of purine with 4-aminopyrimidine-5-carbonitrile or 2-amino-6-methylpyrimidine-5-carbonitrile as HB led to enhancement in PI3Kδ inhibitory activity, this did not transform into the improvement in cellular potency (**21** and **22** versus **14**). Hence, compounds with 4-aminopyrimidine-5-carbonitrile or 2-amino-6-methylpyrimidine-5-carbonitrile as HB were not selected for further evaluation.

Table 2. The anti-proliferative activity of selected compounds against SU-DHL-6 cell line

Cpd.	SU-DHL-6 GI_{50} (nM)	Cpd.	SU-DHL-6 GI_{50} (nM)
14	813	**24**	3417
15	601	**25**	716
16	107	**26**	33
17	937	**27**	945
21	867	**28**	2808
22	1042	**Idelalisib**	34
23	53		

2.4. PI3Kα, β and γ biochemical assays

Table 3. The inhibitory activity of selected compounds against class I PI3K isoforms

Cpd.	PI3Kα IC_{50} (nM)	PI3Kβ IC_{50} (nM)	PI3Kγ IC_{50} (nM)	PI3Kδ IC_{50} (nM)
15	>5000 (>385-fold) [a]	2641 (203-fold) [a]	113 (9-fold) [a]	13
26	221 (221-fold) [a]	174 (174-fold) [a]	4.3 (4-fold) [a]	1.0

a. Selectivity fold

Compounds **15** and **26** were subsequently selected as representatives to identify their inhibitory activities against the other three class I PI3K subtypes. The results demonstrated that both compounds exhibited favorable selectivity over PI3Kα and PI3Kβ (**Table 3**). However, less obvious discrepancy existed between the PI3Kδ and PI3Kγ inhibitory activities of each compound. Therefore, both **15** and

26 were characterized as PI3Kδ/γ dual inhibitors. In particular, compound **26** also exhibited single-digit nanomolar inhibitory activity against PI3Kγ.

2.5. Western blot assay

To confirm its anti-proliferative activity against SU-DHL-6 cell line was resulted from the modulation of PI3K signaling, compound **26**, the most potent compound throughout this series, was then investigated in the Western blot analysis. As illustrated by **Fig. 3**, compound **26** down-regulated both phos-Akt (Ser473) and phos-S6K1 (Thr389), two well-established biomarkers of PI3K signaling, in a dose-dependent manner at 2 h post-treatment. In particular, at the dosage as low as 10 nM, compound **26**-treatment led to dramatic decrease in the phosphoration of both Akt and its downstream signal S6K1. At the dosage of 30 nM, approximately the GI_{50} value of **26**, a more significant decrease in the phosphoration of Akt and S6K1 was observed. As revealed by the immunoblot assay, the anti-proliferative activity of **26** against SU-DHL-6 cell line was attributed to its remarkable capability to attenuate the PI3K signaling.

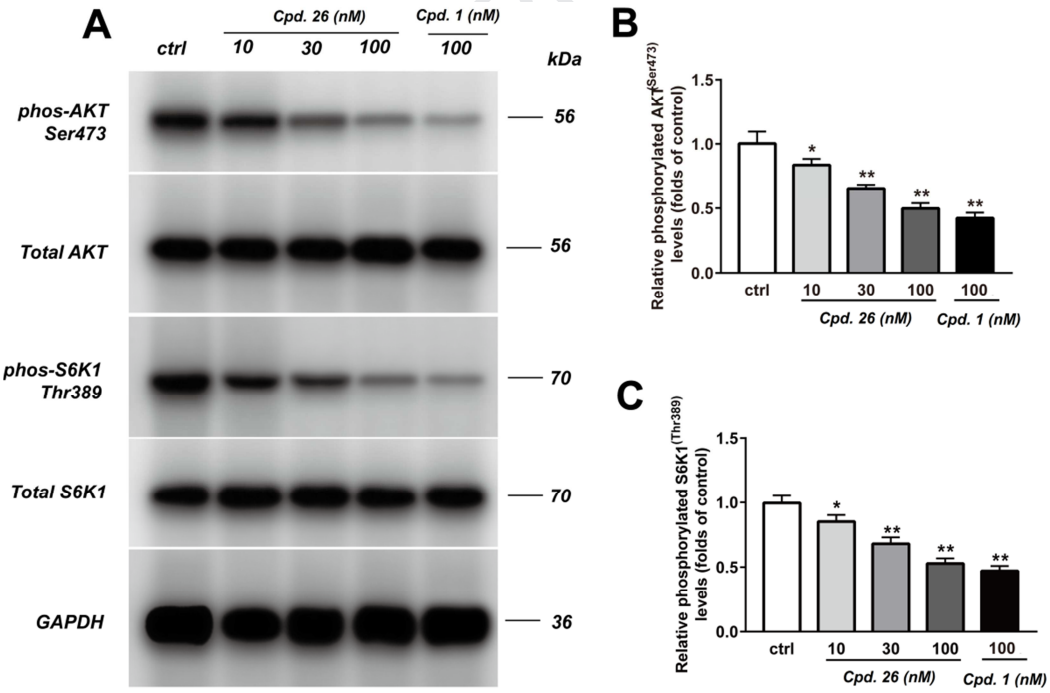

Fig. 3. The capability of compound **26** to attenuate PI3K signaling in SU-DHL-6 cells at 2 h post-treatment: The Akt and S6K1 phosphorylation levels were determined via Western blot assay (A); Phosphorylation levels of Akt (B) and S6K1 (C) were displayed as folds of control with the bar chart indicating the quantification of the bands in immunoblotting (results shown as mean ± SD, n=3). * $p<0.05$, ** $p<0.01$ VS control (cells incubated with the medium alone).

2.6. *In vivo* PK evaluation

The excellent *in vitro* performance of **26** provided an incentive for the further PK study in Sprague–Dawley (SD) rats. Following oral administration at the dosage of 5 mg/kg, compound **26** displayed a high plasma exposure (AUC_{0-t} = 4878 ± 694 h μg/L), an attractive oral bioavailability (F% = 87.5 ± 12.5), and an acceptable clearance (CL = 0.9 ± 0.1 L/h/kg) (**Table 4**). Moreover, it exerted a long elimination half-life ($T_{1/2}$ = 14.3 ± 4.4 h). Given the favorable PK properties, the remarkable *in vitro* potency of **26** was expected to be transformed to favorable therapeutic efficacy *in vivo*.

Table 4. The PK parameters of compound **26**

Cpd.	Route	$T_{1/2}$ (h)[a]	AUC_{0-t} (h μg/L)[a]	Vss (L/kg)[a]	CL (L/h/kg)[a]	F(%)
26	IV (5 mg/kg)	3.0 ± 0.3	5576 ± 606	3.9 ± 0.6	0.9 ± 0.1	87.5 ± 12.5
	PO (5 mg/kg)	14.3 ± 4.4	4878 ± 694	---	---	

a. Data, displayed as mean ± SD, were calculated according to the results of three biological replicates. CL, Vss, $T_{1/2}$, AUC, and F stood for clearance, volume of distribution, half-life, area under the plasma concentration-time curve, and oral bioavailability, respectively.

2.7. Molecular modeling

With the attempt to unravel its possible binding mode with PI3Kδ catalytic cleft, we conducted the molecular docking analysis of **26** on the basis of the disclosed PI3Kδ/Idelalisib co-crystal structure (PDB code 4XE0) [30]. Both Idelalisib (yellow) and compound **26** (magenta) assumed a propeller-shaped conformation with the bicyclic template sandwiched into the hydrophobic selectivity pocket that was induced between Trp760 and Met752 (**Fig. 4A** and **4C**). The 2, 4-diaminopyrimidine-5-carbonitrile moiety, as the HB of **26**, conferred three H-bonds with hinge residues Val828 and Glu826 (**Fig 4B**). Besides, cyclopropyl of the spirocyclic spacer was within the hydrophobic interaction distance of Met752 and Pro758. These potential contacts provided an explanation for the remarkable PI3Kδ inhibitory activity of **26**.

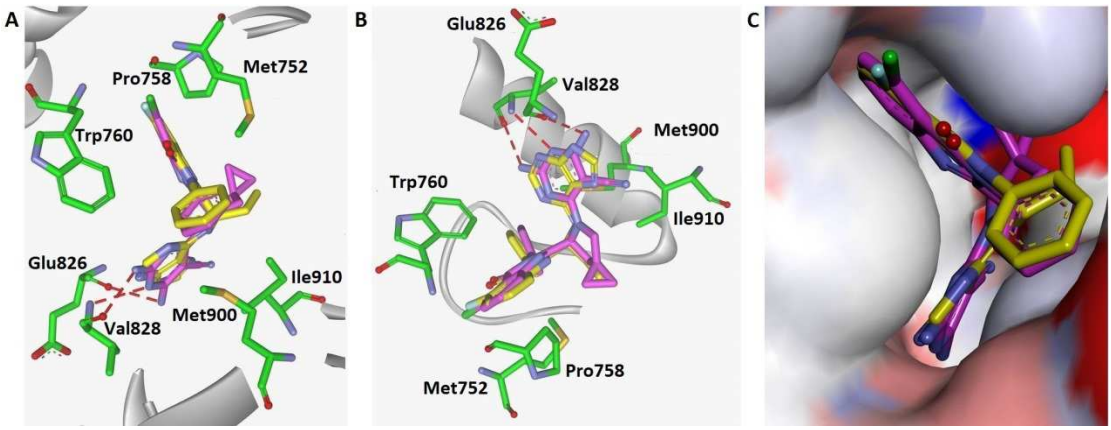

Fig. 4. The molecular docking of compound **26** into the ATP-binding site of PI3Kδ

3. Conclusions

Built upon our insight into the reported propeller-shaped PI3Kδ inhibitors and PI3Kδ/γ dual inhibitors, a novel structural series of quinazolone derivatives were designed and synthesized via incorporation of a seven-membered spirocyclic building block as the spacer between the bicyclic heteroaryl template and HB. The SARs study identified compound **26** as the most potent one throughout this series, which exerted IC_{50} value of 1.0 nM against PI3Kδ, and GI_{50} value of 33 nM against SU-DHL-6 cell line. Besides, it exhibited single-digit nanomolar inhibitory activity against PI3Kγ, along with favorable specificity over PI3Kα and PI3Kβ. Further Western blot analysis illustrated the anti-proliferative potency of **26** was resulted from its remarkable capability to down-regulate PI3K pathway. Importantly, benefiting from its favorable bioavailability (F = 87.5%), the *in vitro* potency of **26** was anticipated to be transformed to desirable *in vivo* therapeutic efficacy. As a promising PI3Kδ/γ dual inhibitor, compound **26** deserves extensive functional investigation to assess its potential as candidate for battling B-cell malignancies.

4. Experimental section

4.1. Chemistry

Chemical reagents used in this work were all purchased from common commercial suppliers. When necessary, purification was performed prior to use. NMR spectra were recorded on a Bruker Avance 400 II (400 MHz) spectrometer after dissolving the samples in DMSO-d_6 or $CDCl_3$. ESI-MS spectra were collected by Bruker Esquire-LC-00075 spectrometer, while ESI-HRMS were obtained by Agilent 6230 TOF LC/MS spectrometer. Silica gel (200–300 mesh) was used for performing flash column chromatography. HPLC was performed using a Shimadzu Essentia LC-16 system with UV detection at

254 nm. Compounds were eluted with a binary solvent system containing A and B [A: CH_3CN; B: H_2O with 0.05% phosphoric acid (W/V)] at the flow rate of 0.8 mL/min. Analytical purity of the target compounds (all over 95%) was presented in the supplementary material.

4.1.1. General procedure for preparing quinazolone derivatives **13a-d**

The mixture of corresponding ortho-amino benzoic acid **12a** (**12b**, **12c** or **12d**, 1.0 eq), (*S*)-5-(*tert*-butoxycarbonyl)-5-azaspiro[2.4]heptane-6-carboxylic acid (1.1 eq), $P(OPh)_3$ (2.5 eq) and pyridine (2 mL/1 mmol substrate) was stirred at 70 °C under N_2 atmosphere. After the total conversion of the ortho-amino benzoic acid, aniline (1.2 eq) was added to the mixture, and the resultant mixture was stirred at the same temperature for 3 h. Following the removal of pyridine in vacuo, the residue was dissolved in EA, and the solvent was washed successively with HCl (1 N), saturated $NaHCO_3$ solution, and brine. The organic layer was dried over anhydrous Na_2SO_4 and concentrated in vacuo. Finally, the residue was subjected to flash column chromatography [petroleum ether (PE)/ethyl acetate (EA) = 40:1-20:1, V/V] to afford the quinazolone derivative (**13a-d**) as pale solid. The ^{1}H NMR spectra of **13a-d** indicated the existence of rotamers.

Tert-butyl (*S*)-6-(5-fluoro-4-oxo-3-phenyl-3,4-dihydroquinazolin-2-yl)-5-azaspiro[2.4]heptane-5-carboxylate (**13a**) Pale solid; yield 53%; ^{1}H NMR (400 MHz, $CDCl_3$): δ 7.77–7.65 (m, 1H), 7.63–7.48 (m, 4H), 7.36 (d, 7.6 Hz, 1H), 7.22–7.09 (m, 2H), 4.75–4.65 (m, 0.4H), 4.63–4.56 (m, 0.6H), 3.78–3.58 (m, 1H), 3.43–3.28 (m 1H), 2.01–1.83 (m, 2H), 1.46 (s, 3H), 1.32 (s, 6H), 0.73–0.62 (m, 1H), 0.61–0.52 (m, 1H), 0.51–0.45 (m, 1H), 0.43–0.35 (m, 1H); ESI-MS: m/z = 436 $[M+H]^+$.

Tert-butyl (*S*)-6-(5-chloro-4-oxo-3-phenyl-3,4-dihydroquinazolin-2-yl)-5-azaspiro[2.4]heptane-5-carboxylate (**13b**) Pale solid; yield 49%; ^{1}H NMR (400 MHz, DMSO-d_6): δ 7.83–7.73 (m, 1H), 7.70–7.53 (m, 5H), 7.52–7.43 (m, 1H), 7.38 (d, 7.6 Hz, 0.4H), 7.29 (d, 7.6 Hz, 0.6H), 4.41–4.29 (m, 1H), 3.55–3.45 (m, 1H), 3.30–3.23 (m, 1H), 2.08–1.92 (m, 1H), 1.90–1.78 (m, 1H), 1.36 (s, 3H), 1.22 (s, 6H), 0.64–0.47 (m, 3H), 0.40–0.28 (m, 1H); ESI-MS: m/z = 452 $[M+H]^+$.

Tert-butyl (*S*)-6-(5-methyl-4-oxo-3-phenyl-3,4-dihydroquinazolin-2-yl)-5-azaspiro[2.4]heptane-5-carboxylate (**13c**) Pale solid; yield 37%; ^{1}H NMR (400 MHz, DMSO-d_6): δ 7.73–7.51 (m, 4H), 7.50–7.40 (m, 2H), 7.39–7.34 (m, 0.4H), 7.33–7.25 (m, 1.6H), 4.41–4.30 (m, 1H), 3.54–3.47 (m, 1H), 3.29–3.21 (m, 1H),

2.78–2.68 (3H, two singlets), 2.04–1.91 (m, 1H), 1.89–1.77 (m, 1H), 1.36 (s, 3H), 1.21 (s, 6H), 0.64–0.46 (m, 3H), 0.39–0.27 (m, 1H); ESI-MS: m/z = 432 $[M+H]^+$.

Tert-butyl (*S*)-6-(6-fluoro-4-oxo-3-phenyl-3,4-dihydroquinazolin-2-yl)-5-azaspiro[2.4]heptane-5-carboxylate (**13d**) Pale solid; yield 54%; ^{1}H NMR (400 MHz, DMSO-d_6): δ 7.86–7.71 (m, 3H), 7.70–7.53 (m, 3H), 7.52–7.44 (m, 1H), 7.39 (d, 8.4 Hz, 0.4H), 7.30 (d, 7.6 Hz, 0.6H), 4.45–4.33 (m, 1H), 3.55–3.46 (m, 1H), 3.31–3.22 (m, 1H), 2.09–1.92 (m, 1H), 1.90–1.78 (m, 1H), 1.36 (s, 3H), 1.20 (s, 6H), 0.66–0.47 (m, 3H), 0.39–0.27 (m, 1H); ESI-MS: m/z = 436 $[M+H]^+$.

4.1.2. General procedure for preparing compounds **14-17**, **21**, **22**, **24**, **25** and **27-29**

To the solution of corresponding quinazolone intermediate **13a** (**13b**, **13c** or **13d**) in DCM (4 mL/1 mmol substrate) was added TFA (1 mL/1 mmol substrate) dropwise at 0 °C, and the resultant mixture was stirred at room temperature. After **13a** (**13b**, **13**c or **13d**) was totally consumed, saturated $NaHCO_3$ solution was added dropwise at 0 °C to adjust the PH value to 7. Following extraction with DCM, the organic layer was washed with brine, dried over anhydrous Na_2SO_4, and concentrated in vacuo to afford the Boc-deprotected secondary amine as slightly yellow solid.

The mixture of corresponding Boc-deprotected secondary amine (1.0 eq), 6-chloro-9*H*-purine (1.5 eq), DIPEA (4.0 eq) and *t*-BuOH (15 mL/1 mmol secondary amine) was stirred at 80 °C under N_2 atmosphere. After the secondary amine was totally consumed, *t*-BuOH was removed in vacuo, and the residue was dissolved in DCM. The solution was washed with saturated $NaHCO_3$ solution, dried over anhydrous Na_2SO_4, and concentrated in vacuo. Finally, the crude product underwent flash column chromatography (DCM/EA = 5:1-1:1, V/V) to afford the purine derivative (**14** or **15-17)** as pale solid. Compounds with 4-aminopyrimidine-5-carbonitrile, 2-amino-6-methylpyrimidine-5-carbonitrile, 2-fluoro-9*H*-purine or 2-chloro-9*H*-purine as HBs were preapred via similar procedure to that for **14-17**. However, the eluents utilized in the final flash column chromatography of **21**, **22**, **24**, **25** and **27** were different (DCM/EA = 15:1-5:1, V/V, for **21**, **24** and **27**; DCM/EA = 20:1-8:1, V/V, for **22** and **25**).The NMR spectra of **14-17**, **28** and **29** indicated the existence of rotamers.

(*S*)-2-(5-(9*H*-purin-6-yl)-5-azaspiro[2.4]heptan-6-yl)-5-fluoro-3-phenylquinazolin-4(3*H*)-one (**14**)

Pale solid; yield 61% (for two steps); ^{1}H NMR (400 MHz, DMSO-d_6): δ 13.00 (s, 0.5H), 12.94 (s, 0.5H), 8.26–8.09 (m, 2H), 7.85–7.46 (m, 6H), 7.35–7.18 (m, 2H), 5.57–5.50 (m, 0.5H), 4.83–4.76 (m, 0.5H), 4.31–4.19 (m, 1H), 3.90 (d, 10.8 Hz, 0.5H), 3.73 (d, 10.8 Hz, 0.5H), 2.21–1.94 (m, 2H), 0.88–

0.76 (m, 1H), 0.68–0.58 (m, 2H), 0.49–0.40 (m, 1H); ^{13}C NMR (100 MHz, DMSO-d_6): δ 161.03 (d, J_{C-F} = 263.0 Hz), 160.96 (d, J_{C-F} = 261.0 Hz), 160.25, 159.29 (d, J_{C-F} = 4.00 Hz), 158.90 (d, J_{C-F} = 5.00 Hz), 158.79, 152.78, 152.62, 152.33, 151.72, 151.47, 150.94, 149.97, 149.55, 139.37, 139.30, 137.07, 136.60, 135.66, 130.69, 130.01, 129.96, 129.90, 129.76, 129.71, 129.57, 129.49, 129.38, 123.84 (d, J_{C-F} = 3.00 Hz), 123.72 (d, J_{C-F} = 3.00 Hz), 119.45, 119.38, 113.34 (d, J_{C-F} = 21.0 Hz), 113.21 (d, J_{C-F} = 19.0 Hz), 110.61 (d, J_{C-F} = 6.00 Hz), 61.54, 60.35, 57.68, 56.36, 38.82, 21.68, 18.94, 13.84, 11.64, 10.85, 8.42; ESI-HRMS: m/z calcd for $C_{25}H_{20}FN_7O$ $[M+H]^+$ 454.1792; found 454.1803; HPLC: t_R = 9.08 min, Agilent TC-C18(2) 250 × 4.6mm 5μm, 30 °C, eluent A-40%, eluent B-60%.

(*S*)-2-(5-(9*H*-purin-6-yl)-5-azaspiro[2.4]heptan-6-yl)-5-chloro-3-phenylquinazolin-4(3*H*)-one (**15**)

Pale solid; yield 66% (for two steps); ^{1}H NMR (400 MHz, DMSO-d_6): δ 12.98 (brs, 1H), 8.28–8.04 (m, 2.5H), 7.81–7.75 (m, 0.5H), 7.73–7.30 (m, 7H), 5.56–5.49 (m, 0.5H), 4.80–4.73 (m, 0.5H), 4.30–4.19 (m, 1H), 3.90 (d, 10.8 Hz, 1H), 3.73 (d, 10.8 Hz, 1H), 2.21–1.92 (m, 2H), 0.89–0.74 (m, 1H), 0.68–0.55 (m, 2H), 0.49–0.40 (m, 1H); ^{13}C NMR (100 MHz, DMSO-d_6): δ 160.32, 159.96, 159.92, 158.48, 152.76, 152.52, 152.22, 151.76, 151.63, 150.96, 150.34, 149.91, 139.77, 139.48, 137.22, 136.75, 134.86, 133.15, 133.11, 130.58, 130.04, 129.98, 129.88, 129.75, 129.70, 129.50, 129.44, 129.32, 129.28, 127.33, 127.22, 119.40, 119.21, 117.91, 61.56, 60.38, 57.63, 56.35, 38.77, 21.64, 18.90, 13.87, 11.67, 10.77, 8.33; ESI-HRMS: m/z calcd for $C_{25}H_{20}ClN_7O$ $[M+H]^+$ 470.1496; found 470.1495; HPLC: t_R = 6.74 min, Agilent TC-C18(2) 250 × 4.6mm 5μm, 30 °C, eluent A-55%, eluent B-45%.

(*S*)-2-(5-(9*H*-purin-6-yl)-5-azaspiro[2.4]heptan-6-yl)-5-methyl-3-phenylquinazolin-4(3*H*)-one (**16**)

Pale solid; yield 59% (for two steps); ^{1}H NMR (400 MHz, DMSO-d_6): δ 8.32–8.00 (m, 2.5H), 7.81–7.44 (m, 5.5H), 7.37–7.11 (m, 2H), 5.67–5.49 (m, 0.5H), 4.86–4.72 (m, 0.5H), 4.31–4.20 (m, 1H), 3.95–3.87 (m, 0.5H), 3.79–3.72 (m, 0.5H), 2.78–2.63 (m, 3H), 2.17–1.92 (m, 2H), 0.85–0.72 (m, 0.5H), 0.69–0.52 (m, 2.5H), 0.49–0.39 (m, 1H); ^{13}C NMR (100 MHz, DMSO-d_6): δ 162.87, 162.50, 158.65, 157.14, 152.82, 152.47, 152.16, 151.96, 151.69, 151.17, 149.42, 149.00, 140.70, 140.62, 139.85, 139.58, 137.66, 137.18, 134.04, 133.98, 130.75, 130.10, 129.92, 129.87, 129.68, 129.63, 129.48, 129.43, 129.31, 129.21, 129.13, 126.02, 125.88, 119.49, 119.43, 119.37, 61.45, 60.24, 57.69, 56.37, 38.97, 23.11, 21.64, 18.89, 14.07, 14.01, 11.74, 10.86, 8.42; ESI-HRMS: m/z calcd for $C_{26}H_{23}N_7O$ $[M+H]^+$ 450.2042; found 450.2035; HPLC: t_R = 12.05 min, Agilent TC-C18(2) 250 × 4.6mm 5μm, 30 °C, eluent A-40%, eluent B-60%.

(*S*)-2-(5-(9*H*-purin-6-yl)-5-azaspiro[2.4]heptan-6-yl)-6-fluoro-3-phenylquinazolin-4(3*H*)-one (**17**)

Pale solid; yield 62% (for two steps); ^{1}H NMR (400 MHz, DMSO-d_6): δ 12.96 (s, 0.5H), 12.90 (s, 0.5H), 8.31–8.04 (m, 2.5H), 7.84–7.72 (m, 1.5H), 7.71–7.46 (m, 6H), 5.63–5.54 (m, 0.5H), 4.88–4.80 (m, 0.5H), 4.33–4.21 (m, 1H), 3.92 (d, 11.2 Hz, 0.5H), 3.76 (d, 11.2 Hz, 0.5H), 2.20–2.08 (m, 1H), 2.04–1.96 (m, 1H), 0.83–0.76 (m, 0.5H), 0.69–0.53 (m, 2.5H), 0.49–0.40 (m, 1H); ^{13}C NMR (100 MHz, DMSO-d_6): δ 161.71 (d, $J_{C\text{-}F}$ = 3.00 Hz), 161.34 (d, $J_{C\text{-}F}$ = 3.00 Hz), 160.40 (d, $J_{C\text{-}F}$ = 244 Hz), 158.58, 157.13, 152.77, 152.62, 152.31, 151.71, 151.44, 150.92, 144.71, 144.29, 139.35, 139.27, 137.25, 136.79, 130.59, 130.54, 130.42, 130.04, 129.98, 129.74, 129.52, 129.45, 129.23, 123.58 (d, $J_{C\text{-}F}$ = 10.0 Hz), 123.34 (d, $J_{C\text{-}F}$ = 10.0 Hz), 122.24, 122.17, 119.45, 119.36, 111.34 (d, $J_{C\text{-}F}$ = 23.0 Hz), 61.51, 60.28, 57.66, 56.35, 38.94, 21.66, 18.90, 13.89, 11.62, 10.83, 8.35; ESI-HRMS: m/z calcd for $C_{25}H_{20}FN_7O$ $[M+H]^+$ 454.1792; found 454.1805; HPLC: t_R = 6.41 min, Agilent TC-C18(2) 250 × 4.6mm 5μm, 30 °C, eluent A-50%, eluent B-50%.

(*S*)-4-amino-6-(6-(5-fluoro-4-oxo-3-phenyl-3,4-dihydroquinazolin-2-yl)-5-azaspiro[2.4]heptan-5-yl) pyrimidine-5-carbonitrile (**21**)

Pale solid; yield 71%; ^{1}H NMR (400 MHz, DMSO-d_6): δ 8.02 (s, 1H), 7.82–7.53 (m, 5H), 7.48 (d, 6.8 Hz, 1H), 7.42 (d, 8.0 Hz, 1H), 7.38–7.02 (m, 3H), 4.79–4.65 (m, 1H), 3.96 (d, 10.0 Hz, 1H), 3.85 (d, 9.6 Hz, 1H), 2.09–1.99 (m, 1H), 1.96–1.86 (m, 1H), 0.79–0.69 (m, 1H), 0.67–0.57 (m, 2H), 0.43–0.35 (m, 1H); ^{13}C NMR (100 MHz, DMSO-d_6): δ 166.12, 161.02 (d, $J_{C\text{-}F}$ = 262 Hz), 159.47, 159.31, 159.11, 158.86 (d, $J_{C\text{-}F}$ = 3.00 Hz), 149.86, 136.85, 135.75 (d, $J_{C\text{-}F}$ = 10.0 Hz), 131.98, 130.00, 129.89, 129.78, 129.35, 123.79 (d, $J_{C\text{-}F}$ = 2.00 Hz), 117.72, 113.32 (d, $J_{C\text{-}F}$ = 19.0 Hz), 110.61 (d, $J_{C\text{-}F}$ = 5.00 Hz), 68.32, 61.63, 56.79, 38.23, 21.48, 12.11, 10.21; ESI-HRMS: m/z calcd for $C_{25}H_{20}FN_7O$ $[M+H]^+$ 454.1792; found 454.1780; HPLC: t_R = 10.97 min, Agilent TC-C18(2) 250 × 4.6mm 5μm, 30 °C, eluent A-50%, eluent B-50%.

(*S*)-2-amino-4-(6-(5-fluoro-4-oxo-3-phenyl-3,4-dihydroquinazolin-2-yl)-5-azaspiro[2.4]heptan-5-yl) -6-methylpyrimidine-5-carbonitrile (**22**)

Pale solid; yield 74%; ^{1}H NMR (400 MHz, DMSO-d_6): δ 7.89 (d, 7.2 Hz, 1H), 7.83–7.72 (m, 1H), 7.68–7.46 (m, 4H), 7.40 (d, 8.0 Hz, 1H), 7.26 (t, 9.2 Hz, 1H), 7.02 (brs, 1H), 6.70 (brs, 1H), 4.86–4.68 (m, 1H), 4.05–3.77 (m, 2H), 2.28 (s, 3H), 1.96–1.77 (m, 2H), 0.73–0.48 (m, 3H), 0.44–0.29 (m, 1H); ^{13}C NMR (100 MHz, DMSO-d_6): δ 172.81, 162.08, 161.06 (d, $J_{C\text{-}F}$ = 261 Hz), 159.81, 159.02, 158.47 (d, $J_{C\text{-}F}$ = 3.00 Hz), 149.78, 136.71, 135.65 (d, $J_{C\text{-}F}$ = 9.00 Hz), 130.18, 129.94, 129.87, 129.73, 129.67, 123.90 (d, $J_{C\text{-}F}$ = 3.00 Hz), 119.87, 113.29 (d, $J_{C\text{-}F}$ = 20.0 Hz), 110.76 (d, $J_{C\text{-}F}$ = 5.00 Hz), 77.92, 61.11,

57.05, 38.18, 23.63, 21.11, 12.92, 9.21; ESI-HRMS: m/z calcd for $C_{26}H_{22}FN_7O$ $[M+H]^+$ 468.1948; found 468.1951; HPLC: t_R = 7.18 min, Agilent TC-C18(2) 250 × 4.6mm 5μm, 30 °C, eluent A-50%, eluent B-50%.

(*S*)-4-amino-6-(6-(5-chloro-4-oxo-3-phenyl-3,4-dihydroquinazolin-2-yl)-5-azaspiro[2.4]heptan-5-yl) pyrimidine-5-carbonitrile (**24**)

Pale solid; yield 70%; ^{1}H NMR (400 MHz, DMSO-d_6): δ 8.02 (s, 1H), 7.75–7.51 (m, 7H), 7.48 (d, 7.2 Hz, 1H), 7.28 (brs, 2H), 4.77–4.64 (m, 1H), 3.95 (d, 9.6 Hz, 1H), 3.86 (d, 9.6 Hz, 1H), 2.08–2.01 (m, 1H), 1.96–1.87 (m, 1H), 0.79–0.68 (m, 1H), 0.65–0.57 (m, 2H), 0.44–0.35 (m, 1H); ^{13}C NMR (100 MHz, DMSO-d_6): δ 166.12, 159.88, 159.30, 159.12, 150.29, 137.08, 134.90, 133.20, 131.98, 130.00, 129.89, 129.75, 129.40, 129.29, 129.13, 127.33, 118.01, 117.73, 68.32, 61.64, 56.81, 38.16, 21.47, 12.27, 10.10; ESI-HRMS: m/z calcd for $C_{25}H_{20}ClN_7O$ $[M+H]^+$ 470.1496; found 470.1503; HPLC: t_R = 11.54 min, Agilent TC-C18(2) 250 × 4.6mm 5μm, 30 °C, eluent A-55%, eluent B-45%.

(*S*)-2-amino-4-(6-(5-chloro-4-oxo-3-phenyl-3,4-dihydroquinazolin-2-yl)-5-azaspiro[2.4]heptan-5-yl) -6-methylpyrimidine-5-carbonitrile (**25**)

Pale solid; yield 68%; ^{1}H NMR (400 MHz, DMSO-d_6): δ 7.89 (d, 7.6 Hz, 1H), 7.71 (t, 8.0 Hz, 1H), 7.65–7.60 (m, 1H), 7.59–7.47 (m, 5H), 7.03 (brs, 1H), 6.70 (brs, 1H), 4.82–4.70 (m, 1H), 3.98–3.84 (m, 2H), 2.28 (s, 3H), 1.94–1.80 (m, 2H), 0.71–0.51 (m, 3H), 0.41–0.32 (m, 1H); ^{13}C NMR (100 MHz, DMSO-d_6): δ 172.80, 162.07, 160.01, 159.78, 158.12, 150.20, 136.93, 134.82, 133.21, 130.18, 129.89, 129.78, 129.69, 129.67, 129.38, 127.44, 119.87, 118.14, 77.90, 61.10, 57.05, 38.05, 23.63, 21.11, 13.05, 9.08; ESI-HRMS: m/z calcd for $C_{26}H_{22}ClN_7O$ $[M+H]^+$ 484.1653; found 484.1666; HPLC: t_R = 9.55 min, Agilent TC-C18(2) 250 × 4.6mm 5μm, 30 °C, eluent A-40%, eluent B-60%.

(*S*)-4-amino-6-(6-(6-fluoro-4-oxo-3-phenyl-3,4-dihydroquinazolin-2-yl)-5-azaspiro[2.4]heptan-5-yl) pyrimidine-5-carbonitrile (**27**)

Pale solid; yield 65%; ^{1}H NMR (400 MHz, DMSO-d_6): δ 8.00 (s, 1H), 7.78 (d, 8.0 Hz, 1H), 7.74–7.44 (m, 7H), 7.21 (brs, 2H), 4.87–4.69 (m, 1H), 4.06–3.91 (m, 1H), 3.86 (d, 10.0 Hz, 1H), 2.06–1.98 (m, 1H), 1.97–1.88 (m, 1H), 0.80–0.69 (m, 1H), 0.67–0.55 (m, 2H), 0.45–0.34 (m, 1H); ^{13}C NMR (100 MHz, DMSO-d_6): δ 166.12, 161.28, 160.48 (d, J_{C-F} = 243 Hz), 159.31, 159.10, 157.83, 144.63, 137.05, 130.60, 130.52, 130.03, 129.91, 129.82, 129.24, 123.56 (d, J_{C-F} = 24.0 Hz), 122.23 (d, J_{C-F} = 8.00 Hz), 117.76, 111.37 (d, J_{C-F} = 24.0 Hz), 68.34, 61.55, 56.80, 38.34, 21.48, 12.10, 10.20; ESI-HRMS: m/z calcd for $C_{25}H_{20}FN_7O$ $[M+H]^+$ 454.1792; found 454.1785; HPLC: t_R = 11.75 min, Agilent TC-C18(2)

250 × 4.6mm 5μm, 30 °C, eluent A-55%, eluent B-45%.

(*S*)-5-chloro-2-(5-(2-fluoro-9*H*-purin-6-yl)-5-azaspiro[2.4]heptan-6-yl)-3-phenylquinazolin-4(3H)-one (**28**)

Pale solid; yield 67%; ^{1}H NMR (400 MHz, DMSO-d_6): δ 14.12 (brs, 0.2H), 13.16 (s, 0.4H), 13.08 (s, 0.4H), 8.70 (s, 0.4H), 8.27–8.01 (m, 1.6H), 7.77–7.33 (m, 7H), 5.57–5.48 (m, 0.5H), 4.77–4.69 (m, 0.5H), 4.31–4.19 (m, 1H), 3.84 (d, 11.2 Hz, 0.5H), 3.68 (d, 11.2 Hz, 0.5H), 2.21–2.01 (m, 2H), 0.88–0.74 (m, 1H), 0.71–0.55 (m, 2H), 0.49–0.40 (m, 1H); ^{13}C NMR (100 MHz, DMSO-d_6): δ 160.25, 159.85, 159.05, 158.71 (d, J_{C-F} = 200 Hz), 158.24 (d, J_{C-F} = 202 Hz), 157.87, 154.13, 153.92, 152.32, 152.12, 150.24, 149.86, 139.95, 139.88, 139.86, 137.12, 136.71, 134.92, 134.83, 133.24, 133.15, 130.67, 130.15, 130.08, 129.88, 129.79, 129.76, 129.74, 129.53, 129.38, 129.13, 129.02, 127.41, 127.29, 117.99 (d, J_{C-F} = 2.00 Hz), 117.93 (d, J_{C-F} = 4.00 Hz), 117.86 (d, J_{C-F} = 4.00 Hz), 61.68, 60.65, 60.22, 57.73, 56.54, 38.50, 21.52, 18.82, 13.85, 12.08, 10.24, 8.07; ESI-HRMS: m/z calcd for $C_{25}H_{19}ClFN_7O$ $[M+H]^+$ 488.1402; found 488.1416; HPLC: t_R = 7.37 min, Agilent TC-C18(2) 250 × 4.6mm 5μm, 30 °C, eluent A-70%, eluent B-30%.

(*S*)-5-chloro-2-(5-(2-chloro-9*H*-purin-6-yl)-5-azaspiro[2.4]heptan-6-yl)-3-phenylquinazolin-4(3*H*)-one (**29**)

Pale solid; yield 62%; ^{1}H NMR (400 MHz, DMSO-d_6): δ 14.14 (brs, 0.2H), 13.21 (s, 0.4H), 13.13 (s, 0.4H), 8.74 (s, 0.6H), 8.32–8.04 (m, 1.4H), 7.86–7.79 (m, 0.5H), 7.77–7.42 (m, 6H), 7.39 (dd, 1.5 Hz, 8.4 Hz, 0.5H), 5.53–5.46 (m, 0.4H), 4.78–4.69 (m, 0.6H), 4.29–4.16 (m, 1H), 3.85 (d, 11.2 Hz, 0.5H), 3.69 (d, 11.2 Hz, 0.5H), 2.18–1.94 (m, 2H), 0.91–0.71 (m, 1H), 0.69–0.56 (m, 2H), 0.51–0.39 (m, 1H); ^{13}C NMR (100 MHz, DMSO-d_6): δ 160.25, 159.83, 159.04, 157.88, 153.25, 153.05, 152.53, 151.97, 151.23, 150.26, 149.85, 148.19, 140.08, 137.16, 136.71, 134.91, 134.82, 133.23, 133.14, 130.66, 130.16, 130.06, 129.88, 129.79, 129.78, 129.73, 129.52, 129.48, 129.35, 129.32, 127.41, 127.29, 118.48, 117.97, 61.69, 60.59, 57.73, 56.56, 38.45, 21.46, 18.85, 13.84, 12.25, 10.10, 8.05; ESI-HRMS: m/z calcd for $C_{25}H_{19}Cl_2N_7O$ $[M+H]^+$ 504.1106; found 504.1098; HPLC: t_R = 9.06 min, Agilent TC-C18(2) 250 × 4.6mm 5μm, 30 °C, eluent A-40%, eluent B-60%.

4.1.3. General procedure for preparing compounds **23** and **26**

The mixture of corresponding Boc-deprotected secondary amine obtained in section 4.1.2 (1.1 eq), 2, 4-diamino-6-chloropyrimidine-5-carbonitrile (1.0 eq), DIPEA (5.5 eq), KF (2.0 eq) and DMSO (10 mL/1 mmol substrate) was stirred at 90 °C under N_2 atmosphere. After the total consumption of 2,

4-diamino-6-chloropyrimidine-5-carbonitrile, water was added to the mixture, and the crude product was obtained via filtration. Finally, the crude product underwent flash column chromatography (DCM/EA = 10:1-4:1, V/V) to afford the title compound as pale solid.

(*S*)-2,4-diamino-6-(6-(5-fluoro-4-oxo-3-phenyl-3,4-dihydroquinazolin-2-yl)-5-azaspiro[2.4]heptan-5-yl)pyrimidine-5-carbonitrile (**23**)

Pale solid; yield 51%; ^{1}H NMR (400 MHz, DMSO-d_6): δ 7.87 (d, 6.8 Hz, 1H), 7.82–7.72 (m, 1H), 7.67–7.39 (m, 5H), 7.26 (t, 9.2 Hz, 1H), 6.50 (brs, 2H), 6.21 (brs, 2H), 4.89–4.68 (m, 1H), 3.97–3.75 (m, 2H), 1.95–1.76 (m, 2H), 0.71–0.50 (m, 3H), 0.43–0.29 (m, 1H); ^{13}C NMR (100 MHz, DMSO-d_6): δ 166.99, 162.46, 161.06 (d, $J_{C\text{-}F}$ = 262.0 Hz), 160.98, 159.07, 159.00 (d, $J_{C\text{-}F}$ = 4.00 Hz), 149.88, 136.75, 135.62 (d, $J_{C\text{-}F}$ = 11.0 Hz), 130.12, 129.90, 129.79, 129.64 (d, $J_{C\text{-}F}$ = 2.00 Hz), 123.88 (d, $J_{C\text{-}F}$ = 3.00 Hz), 120.02, 113.19 (d, $J_{C\text{-}F}$ = 20.0 Hz), 110.75, 110.70, 60.90, 60.82, 57.07, 38.36, 20.93, 12.87, 9.40; ESI-HRMS: m/z calcd for $C_{25}H_{21}FN_8O$ $[M+H]^+$ 469.1901; found 469.1916; HPLC: t_R = 7.26 min, Agilent TC-C18(2) 250 × 4.6mm 5μm, 30 °C, eluent A-40%, eluent B-60%.

(*S*)-2,4-diamino-6-(6-(5-chloro-4-oxo-3-phenyl-3,4-dihydroquinazolin-2-yl)-5-azaspiro[2.4]heptan-5-yl)pyrimidine-5-carbonitrile (**26**)

Pale solid; yield 54%; ^{1}H NMR (400 MHz, DMSO-d_6): δ 7.87 (d, 7.2 Hz, 1H), 7.71 (t, 8.0 Hz, 1H), 7.66–7.38 (m, 6H), 6.55 (brs, 2H), 6.25 (brs, 2H), 4.84–4.69 (m, 1H), 3.86 (s, 2H), 1.93–1.73 (m, 2H), 0.68–0.51 (m, 3H), 0.41–0.28 (m, 1H); ^{13}C NMR (100 MHz, DMSO-d_6): δ 166.96, 162.40, 160.96, 160.03, 158.75, 150.29, 136.98, 134.80, 133.19, 130.12, 129.89, 129.64, 129.31, 127.45, 120.02, 118.10, 60.92, 60.83, 57.09, 38.29, 20.99, 13.03, 9.28; ESI-HRMS: m/z calcd for $C_{25}H_{21}ClN_8O$ $[M+H]^+$ 485.1605; found 485.1622; HPLC: t_R = 7.83 min, Agilent TC-C18(2) 250 × 4.6mm 5μm, 30 °C, eluent A-50%, eluent B-50%.

4.1.4. General procedure for preparing amide intermediates **31a-c**

The mixture of 2-fluoro-6-nitrobenzoic acid (1.0 eq), catalytic amount of DMF, and $SOCl_2$ (0.5 mL/1 mmol substrate) was refluxed for 5 h. Afterwards, it was concentrated, and the residue was dissolved in anhydrous DCM. The resultant solution was added dropwise to a solution of corresponding amine (1.0 eq) and TEA (1.2 eq) in anhydrous DCM at 0 °C. After being stirred at room temperature for 3 h, the reaction mixture was quenched by saturated $NaHCO_3$ solution, and extracted with DCM. The organic layer was washed with brine, dried over anhydrous Na_2SO_4, and concentrated in vacuo. Finally, the crude product underwent flash column chromatography (PE/EA = 5:1, V/V) to

afford the amide (**31a**, **31b** or **31c**) as slight yellow solid.

N-benzyl-2-fluoro-6-nitrobenzamide (**31a**) Slight yellow solid; yield 61%.

N-cyclopentyl-2-fluoro-6-nitrobenzamide (**31b**) Slight yellow solid; yield 74%.

N- cyclohexyl-2-fluoro-6-nitrobenzamide (**31c**) Slight yellow solid; yield 71%.

4.1.5. General procedure for preparing imide intermediates **32a-c**

The mixture of corresponding amide (**31a**, **31b** or **31c**, 1.0 eq), catalytic amount of DMF, and $SOCl_2$ (3 mL/1 mmol amide) was stirred at 80 °C under N_2 atmosphere for 2 h. Afterwards, it was concentrated in vacuo, and the residue was dissolved in anhydrous DCM (6 mL/1 mmol amide). The resultant mixture was added dropwise to a solution of (*S*)-5-(*tert*-butoxycarbonyl)-5-azaspiro[2.4]heptane-6-carboxylic acid (1.1 eq) and anhydrous TEA (3.0 eq) in anhydrous DCM (6 mL/1 mmol amide) at 0 °C under N_2 atmosphere. After being stirred at the same temperature for 1 h, the reaction mixture was stirred at room temperature for 6 h. Then, it was quenched by saturated $NaHCO_3$ solution and extracted with DCM. The organic layer was washed with brine, dried over anhydrous Na_2SO_4, and concentrated in vacuo. Finally, the residue underwent flash column chromatography (PE/EA = 4:1, V/V) to afford the imide (**32a**, **32b** or **32c**) as slightly brown foam or pale foam. The ^{1}H NMR spectra of **32a-c** indicated the existence of rotamers.

Tert-butyl (*S*)-6-(benzyl(2-fluoro-6-nitrobenzoyl)carbamoyl)-5-azaspiro[2.4]heptane-5-carboxylate (**32a**)

Slightly brown foam; yield 45%; ^{1}H NMR (400 MHz, DMSO-d_6): δ 8.27–8.15 (m, 1H), 7.93–7.73 (m, 2H), 7.64–7.08 (m, 5H), 5.45–4.70 (m, 3H), 3.29–3.06 (m, 2H), 2.45–2.22 (m, 1H), 1.64–1.43 (m, 1H), 1.40–1.15 (9H, three singlets), 0.61–0.36 (m, 3H), 0.34–0.21 (m, 1H); ESI-MS: m/z = 498 $[M+H]^+$.

Tert-butyl (*S*)-6-(cyclopentyl(2-fluoro-6-nitrobenzoyl)carbamoyl)-5-azaspiro[2.4]heptane-5-carboxylate (**32b**)

Pale foam; yield 53%; ^{1}H NMR (400 MHz, DMSO-d_6): δ 8.22–8.11 (m, 1H), 7.91–7.84 (m, 1H), 7.81–7.70 (m, 1H), 5.24–5.08 (m, 1H), 4.56–4.33 (m, 1H), 3.40–3.36 (m, 1H), 3.12 (d, 10.0 Hz, 1H), 2.63–2.56 (m, 0.7H), 2.49–2.41 (m, 0.3H), 2.16–1.72 (m, 6H), 1.63–1.43 (m, 3H), 1.39–1.28 (9H, three singlets), 0.61–0.39 (m, 3H), 0.38–0.24 (m, 1H); ESI-MS: m/z = 476 $[M+H]^+$.

Tert-butyl (*S*)-6-(cyclohexyl(2-fluoro-6-nitrobenzoyl)carbamoyl)-5-azaspiro[2.4]heptane-5-carboxylate (**32c**)

Pale foam; yield 56%; ^{1}H NMR (400 MHz, DMSO-d_6): δ 8.22–8.10 (m, 1H), 7.89–7.81 (m, 1H), 7.79–7.70 (m, 1H), 5.16–5.00 (m, 1H), 3.91–3.69 (m, 1H), 3.28–3.25 (m, 1H), 3.17–3.04 (m, 1H), 2.71–2.54 (m, 1H), 2.42–2.23 (m, 2H), 1.86–1.66 (m, 4H), 1.65–1.45 (m, 2H), 1.40–1.26 (11H), 1.18–1.06 (m, 1H), 0.63–0.51 (m, 2H), 0.50–0.23 (m, 2H); ESI-MS: m/z = 490 $[M+H]^+$.

4.1.6. General procedure for preparing quinazolone intermediates **33a-c**

To a solution of corresponding imide (**32a**, **32b** or **32c**, 1.0 eq) in AcOH (10 mL/1 mmol imide) was carefully added activated zinc powder (10 eq) at room temperature. The resultant mixture was sttired at 40 °C under N_2 atmosphere for 8 h. After filtration, the filtrate was concentrated in vacuo, and the residue was dissolved in DCM. Then, the solution was washed with saturated $NaHCO_3$ solution and brine. The organic layer was dried over anhydrous Na_2SO_4, and concentrated in vacuo. Finally, the residue underwent flash column chromatography (PE/EA = 6:1, V/V) to afford the quinazolone derivative (**33a**, **33b** or **33c**) as white foam. The ^{1}H NMR spectra of **33a-c** indicated the existence of rotamers.

Tert-butyl (*S*)-6-(3-benzyl-5-fluoro-4-oxo-3,4-dihydroquinazolin-2-yl)-5-azaspiro[2.4]heptane-5-carboxylate (**33a**)

White foam; yield 83%; ^{1}H NMR (400 MHz, DMSO-d_6): δ 7.87–7.76 (m, 1H), 7.42 (d, 8.0 Hz, 1H), 7.39–7.23 (m, 6H), 5.47–5.20 (m, 2H), 5.10–4.98 (m, 1H), 3.57–3.47 (m, 1H), 3.41–3.37 (m, 0.3H), 3.32–3.26 (m, 0.7H), 1.44–1.21 (m, 5H), 1.06 (s, 6H), 0.61–0.51 (m, 2H), 0.43–0.35 (m, 2H); ESI-MS: m/z = 450 $[M+H]^+$.

Tert-butyl (*S*)-6-(3-cyclopentyl-5-fluoro-4-oxo-3,4-dihydroquinazolin-2-yl)-5-azaspiro[2.4]heptane-5-carboxylate (**33b**)

White foam; yield 72%; ^{1}H NMR (400 MHz, $CDCl_3$): δ 7.68–7.53 (m, 1H), 7.47–7.35 (m, 1H), 7.16–7.01 (m, 1H), 5.35–5.25 (m, 0.4H), 5.24–5.14 (m, 0.6H), 4.69–4.46 (m, 1H), 3.69 (d, 10.0 Hz, 0.7H), 3.61–3.48 (m, 1.3H), 2.54–2.37 (m, 2H), 2.26–2.08 (m, 2H), 2.00–1.92 (m, 1H), 1.85–1.75 (m, 1H), 1.74–1.57 (m, 4H), 1.49 (s, 3H), 1.30–1.15 (m, 6H), 0.75–0.53 (m, 3H), 0.52–0.34 (m, 1H); ESI-MS: m/z = 428 $[M+H]^+$.

Tert-butyl (*S*)-6-(3-cyclohexyl-5-fluoro-4-oxo-3,4-dihydroquinazolin-2-yl)-5-azaspiro[2.4]heptane-5-carboxylate

(**33c**)

White foam; yield 84%; ^{1}H NMR (400 MHz, DMSO-d_6): δ 7.82–7.70 (m, 1H), 7.32 (d, 8.4 Hz, 1H), 7.27–7.15 (m, 1H), 5.25–5.09 (m, 1H), 4.13–3.86 (m, 1H), 3.59–3.37 (m, 2H), 2.75–2.54 (m, 2H), 1.87–1.71 (m, 4H), 1.69–1.58 (m, 2H), 1.57–1.43 (m, 1H), 1.41–1.16 (m, 6H), 1.10 (s, 6H), 0.70-0.39 (m, 4H); ESI-MS: m/z = 442 $[M+H]^+$.

4.1.7. General procedure for preparing target compounds **18-20**

Compounds **18-20** were prepared via similar procedure to that for compounds **14-17** as pale solid. The NMR spectra of **18-20** indicated the existence of rotamers.

(*S*)-2-(5-(9*H*-purin-6-yl)-5-azaspiro[2.4]heptan-6-yl)-3-benzyl-5-fluoroquinazolin-4(3*H*)-one (**18**)

Pale solid; yield 57% (for two steps); ^{1}H NMR (400 MHz, DMSO-d_6): δ 8.29–7.83 (m, 2H), 7.76–7.61 (m, 1H), 7.60–7.07 (m, 7H), 6.32–6.20 (m, 0.4H), 5.82–5.67 (m, 0.6H), 5.64–5.41 (m, 2H), 4.36 (d, 10.0 Hz, 0.5H), 4.23 (d, 11.2 Hz, 0.5H), 3.99–3.88 (m, 0.5H), 3.79–3.70 (m, 0.5H), 2.29–2.02 (m, 1.3H), 1.95–1.85 (m, 0.7H), 0.79–0.21 (m, 4H); ^{13}C NMR (100 MHz, DMSO-d_6): δ 160.82 (d, $J_{C\text{-}F}$ = 261.0 Hz), 160.32, 158.98, 152.18, 151.85, 151.77, 149.57, 140.17, 136.96, 135.54 (d, $J_{C\text{-}F}$ = 10.0 Hz), 128.96, 127.70, 127.43, 123.67, 119.47, 113.19 (d, $J_{C\text{-}F}$ = 20.0 Hz), 109.99 (d, $J_{C\text{-}F}$ = 6.00 Hz), 60.28, 57.64, 46.33, 39.04, 24.78, 21.49, 18.82, 12.02, 10.39; ESI-HRMS: m/z calcd for $C_{26}H_{22}FN_7O$ $[M+H]^+$ 468.1948; found 468.1942; HPLC: t_R = 9.54 min, Agilent TC-C18(2) 250 × 4.6mm 5μm, 30 °C, eluent A-40%, eluent B-60%.

(*S*)-2-(5-(9*H*-purin-6-yl)-5-azaspiro[2.4]heptan-6-yl)-3-cyclopentyl-5-fluoroquinazolin-4(3*H*)-one (**19**)

Pale solid; yield 60% (for two steps); ^{1}H NMR (400 MHz, $CDCl_3$): δ 13.17 (brs, 1H), 8.44 (s, 0.6H), 8.18 (s, 0.4H), 8.00 (s, 0.4H), 7.69 (s, 0.6H), 7.54–7.36 (m, 1H), 7.20 (d, 8.0 Hz, 0.4H), 7.14 (d, 8.0 Hz, 0.6H), 7.06–6.91 (m, 1H), 6.72–6.57 (m, 0.6H), 5.97–5.86 (m, 0.4H), 4.96–4.77 (m, 1H), 4.54 (d, 10.8 Hz, 0.4H), 4.44 (d, 10.8 Hz, 0.4H), 4.13 (d, 10.8 Hz, 0.6H), 3.97 (d, 10.8 Hz, 0.6H), 2.63–2.30 (m, 3H), 2.29–2.11 (m, 2H), 1.93–1.65 (m, 5H), 0.87–0.64 (m, 3H), 0.61–0.40 (m, 1H); ^{13}C NMR (100 MHz, DMSO-d_6): δ 160.73 (d, $J_{C\text{-}F}$ = 262.0 Hz), 159.97, 158.93 (d, $J_{C\text{-}F}$ = 3.00 Hz), 152.83, 152.56, 151.09, 149.02, 139.18, 134.92 (d, $J_{C\text{-}F}$ = 10.0 Hz), 123.37, 119.72, 112.88 (d, $J_{C\text{-}F}$ = 21.0 Hz), 110.89 (d, $J_{C\text{-}F}$ = 5.00 Hz), 61.74, 58.57, 56.12, 39.03, 28.92, 28.30, 26.19, 26.08, 19.04, 14.82, 8.24; ESI-HRMS: m/z calcd for $C_{24}H_{24}FN_7O$ $[M+H]^+$ 446.2105; found 446.2108; HPLC: t_R = 6.94 min, Agilent TC-C18(2) 250 × 4.6mm 5μm, 30 °C, eluent A-50%, eluent B-50%.

(*S*)-2-(5-(9*H*-purin-6-yl)-5-azaspiro[2.4]heptan-6-yl)-3-cyclohexyl-5-fluoroquinazolin-4(3*H*)-one (**20**)

Pale solid; yield 63% (for two steps); ^{1}H NMR (400 MHz, DMSO-d_6): δ 12.99 (s, 0.3H), 12.86 (s, 0.7H), 8.31–7.86 (m, 2H), 7.69–7.51 (m, 1H), 7.22–7.00 (m, 2H), 6.49–6.32 (m, 0.7H), 5.85–5.72 (m, 0.3H), 4.47 (d, 11.2 Hz, 0.3H), 4.40–4.16 (m, 1.3H), 4.02 (d, 10.8 Hz, 0.7H), 3.76 (d, 10.8 Hz, 0.7H), 3.00–2.84 (m, 0.7H), 2.80–2.56 (m, 2.3H), 2.49–2.43 (m, 1H), 2.15–1.33 (m, 8H), 0.78–0.42 (m, 4H); ^{13}C NMR (100 MHz, DMSO-d_6): δ 160.73 (d, $J_{C\text{-}F}$ = 263.0 Hz), 159.60 (d, $J_{C\text{-}F}$ = 4.00 Hz), 159.33, 152.89, 152.67, 150.87, 149.19, 148.93, 139.31, 138.94, 134.98 (d, $J_{C\text{-}F}$ = 10.0 Hz), 123.38, 123.28, 119.59, 113.96 (d, $J_{C\text{-}F}$ = 21.0 Hz), 111.03 (d, $J_{C\text{-}F}$ = 4.00 Hz), 61.70, 60.12, 59.71, 57.82, 56.21, 38.81, 28.27, 27.89, 26.34, 26.19, 26.05, 25.61, 25.47, 18.93, 14.80, 10.27, 8.25; ESI-HRMS: m/z calcd for $C_{25}H_{26}FN_7O$ $[M+H]^+$ 460.2261; found 460.2267; HPLC: t_R = 11.43 min, Agilent TC-C18(2) 250 × 4.6mm 5μm, 30 °C, eluent A-50%, eluent B-50%.

4.2. Biology

4.2.1. Class I PI3Ks biochemical assay

The inhibitory activity against class I PI3Ks was evaluated via ADP-Glo assay according to a reported protocol with minor modification [35].

4.2.2. Anti-proliferative assay

The anti-proliferative activity of compounds against SU-DHL-6 cell line was evaluated via MTT assay. SU-DHL-6 cells (ATCC) seeded in 96-well plates at the density of 1×10^5/well were cultured (37 °C, 5% CO_2) till 90% of the cells were fused. Following 2 h-incubation in serum-free medium, the supernatant was discarded. The cells were incubated with RPMI 1640 medium alone or with the tested compounds at the indicated concentrations for 72 h. At 68 h post-compound treatment, 20 μL MTT solution (5 mg/mL) was added. The 96-well plates were centrifuged at 1500 rpm for 3 min, and the supernatant was discarded. After adding 150 μL DMSO to each well, the plates were shaken for 10 min. The OD_{570} value was read and the inhibition rates calculated accordingly. GI_{50} values were calculated using GraphPad Prism 6.

4.2.3. Western blot assay

Anti-phos-Akt (S473), Anti-Akt, Anti-phos-S6K1 (T389), Anti-S6K1, and Anti-GAPDH purchased from Abcam Inc., as well as corresponding secondary antibodies were utilized in Western blot analysis. GAPDH served as a loading control. SU-DHL-6 cells seeded into six-well plate at a density of 1 ×

10^6/well were cultured overnight (37 °C, 5% CO_2). Following exposure to compound **26** or Idelalisib at the desired concentrations for 2 h, cells were harvested for immunoblotting. The proteins were separated on SDS-PAGE, and subsequently transferred onto PVDF membrane. After successive incubation of the membranes with antibodies and secondary antibodies, the membranes were imaged and the optical density measured.

4.2.4. PK study

The dosage and the number of animals for each group were presented in **Table 4**. Male SD rats were used in this experiment. Both the intravenous and oral doses were formulated in a solution of 5% DMSO, 10% Solutol, 10% EtOH and 75% Saline. At the designated time points, the animal was anaesthetized with isoflurane, and blood sample was collected via ophthalmic vein for terminal bleeding into heparin-coated EP tubes. The plasma samples were stored at –20 °C till the analysis, and the concentration of the tested compound in plasma was determined with UHPLC-MS/MS.

4.3. Molecular docking

C-DOCKER module of Discovery Studio (version 2.5; Accelrys, San Diego, CA, USA, 2008) was utilized for the molecular modeling. The CHARMm-force field was applied to the protein after the removal of original ligand and solvent molecules from the PI3Kδ/Idelalisib co-crystal structure. 3D structure of the ligand was generated, and the energy minimization performed. The ligand was then docked into the active site of the receptor, which was defined according to the location of Idelalisib in the enzyme. The ultimate binding conformation was determined on the basis of the calculated C-DOCKING ENERGE.

Conflict of interest

The authors confirm that this article content has no conflicts of interest.

Acknowledgements

This research was financially spported by Natural Science Foundation of Anhui Province (No. 1808085QH261 and 1808085QH289), the Key Project of Natural Science Research in Universities of Anhui Province (No. KJ2019A1004), and University-Enterprise Cooperative Projects (No. 2018HZ6 and No. 2019HZ078).

References

[1] L. Liu; K. D. Puri; J. M. Penninger; P. Kubes, Leukocyte PI3Kgamma and PI3Kdelta have temporally distinct roles for leukocyte recruitment in vivo. *Blood* **2007,** *110* (4), 1191-1198.

[2] K. Okkenhaug; K. Ali; B. Vanhaesebroeck, Antigen receptor signalling: a distinctive role for the p110delta isoform of PI3K. *Trends Immunol* **2007,** *28* (2), 80-87.

[3] B. S. Kahl; S. E. Spurgeon; R. R. Furman; I. W. Flinn; S. E. Coutre; J. R. Brown; D. M. Benson; J. C. Byrd; S. Peterman; Y. Cho; A. Yu; W. R. Godfrey; N. D. Wagner-Johnston, A phase 1 study of the PI3Kdelta inhibitor idelalisib in patients with relapsed/refractory mantle cell lymphoma (MCL). *Blood* **2014,** *123* (22), 3398-3405.

[4] C. Jimenez; C. Hernandez; B. Pimentel; A. C. Carrera, The p85 regulatory subunit controls sequential activation of phosphoinositide 3-kinase by Tyr kinases and Ras. *J Biol Chem* **2002,** *277* (44), 41556-41562.

[5] B. Bartok; D. L. Boyle; Y. Liu; P. Ren; S. T. Ball; W. D. Bugbee; C. Rommel; G. S. Firestein, PI3 kinase delta is a key regulator of synoviocyte function in rheumatoid arthritis. *Am J Pathol* **2012,** *180* (5), 1906-1916.

[6] W. C. Rowan; J. L. Smith; K. Affleck; A. Amour, Targeting phosphoinositide 3-kinase delta for allergic asthma. *Biochem Soc Trans* **2012,** *40* (1), 240-245.

[7] A. K. Stark; S. Sriskantharajah; E. M. Hessel; K. Okkenhaug, PI3K inhibitors in inflammation, autoimmunity and cancer. *Curr Opin Pharmacol* **2015,** *23*, 82-91.

[8] J. Ball; S. Archer; S. Ward, PI3K inhibitors as potential therapeutics for autoimmune disease. *Drug Discov Today* **2014,** *19* (8), 1195-1199.

[9] X. Wang; X. Zhang; B. S. Li; X. Zhai; Z. Yang; L. X. Ding; H. Wang; C. Liang; W. Zhu; J. Ding; L. H. Meng, Simultaneous targeting of PI3Kdelta and a PI3Kdelta-dependent MEK1/2-Erk1/2 pathway for therapy in pediatric B-cell acute lymphoblastic leukemia. *Oncotarget* 2014, *5* (21), 10732-10744.

[10] Q. Yang; P. Modi; T. Newcomb; C. Queva; V. Gandhi, Idelalisib: First-in-Class PI3K Delta Inhibitor for the Treatment of Chronic Lymphocytic Leukemia, Small Lymphocytic Leukemia, and Follicular Lymphoma. *Clin Cancer Res* **2015,** *21* (7), 1537-1542.

[11] C. Deng; M. R. Lipstein; L. Scotto; X. O. Jirau Serrano; M. A. Mangone; S. Li; J. Vendome; Y. Hao; X. Xu; S. X. Deng; R. B. Realubit; N. P. Tatonetti; C. Karan; S. Lentzsch; D. A. Fruman; B.

Honig; D. W. Landry; O. A. O'Connor, Silencing c-Myc translation as a therapeutic strategy through targeting PI3Kdelta and CK1epsilon in hematological malignancies. *Blood* **2017,** *129* (1), 88-99.

[12] N. Shin; Y. L. Li; S. Mei; K. H. Wang; L. Hall; K. Katiyar; Q. Wang; G. Yang; B. Rumberger; L. Leffet; X. He; M. Rupar; K. Bowman; M. Favata; J. Li; M. Liu; Y. Li; M. Covington; H. Koblish; M. Soloviev; D. Shuey; T. Burn; S. Diamond; J. Fridman; A. Combs; W. Yao; S. Yeleswaram; G. Hollis; K. Vaddi; R. Huber; R. Newton; P. Scherle, INCB040093 Is a Novel PI3Kdelta Inhibitor for the Treatment of B Cell Lymphoid Malignancies. *J Pharmacol Exp Ther* **2018,** *364* (1), 120-130.

[13] M. W. D. Perry; R. Abdulai; M. Mogemark; J. Petersen; M. J. Thomas; B. Valastro; A. Westin Eriksson, Evolution of PI3Kgamma and delta Inhibitors for Inflammatory and Autoimmune Diseases. *J Med Chem* **2019,** *62* (10), 4783-4814.

[14] R. A. Allen; D. C. Brookings; M. J. Powell; J. Delgado; L. K. Shuttleworth; M. Merriman; I. J. Fahy; R. Tewari; J. P. Silva; L. J. Healy; G. C. G. Davies; B. Twomey; R. M. Cutler; A. Kotian; A. Crosby; G. McCluskey; G. F. Watt; A. Payne, Seletalisib: Characterization of a Novel, Potent, and Selective Inhibitor of PI3Kdelta. *J Pharmacol Exp Ther* **2017,** *361* (3), 429-440.

[15] K. Hoegenauer; N. Soldermann; F. Zecri; R. S. Strang; N. Graveleau; R. M. Wolf; N. G. Cooke; A. B. Smith; G. J. Hollingworth; J. Blanz; S. Gutmann; G. Rummel; A. Littlewood-Evans; C. Burkhart, Discovery of CDZ173 (Leniolisib), Representing a Structurally Novel Class of PI3K Delta-Selective Inhibitors. *ACS Med Chem Lett* **2017,** *8* (9), 975-980.

[16] K. Down; A. Amour; I. R. Baldwin; A. W. Cooper; A. M. Deakin; L. M. Felton; S. B. Guntrip; C. Hardy; Z. A. Harrison; K. L. Jones; P. Jones; S. E. Keeling; J. Le; S. Livia; F. Lucas; C. J. Lunniss; N. J. Parr; E. Robinson; P. Rowland; S. Smith; D. A. Thomas; G. Vitulli; Y. Washio; J. N. Hamblin, Optimization of Novel Indazoles as Highly Potent and Selective Inhibitors of Phosphoinositide 3-Kinase delta for the Treatment of Respiratory Disease. *J Med Chem* **2015,** *58* (18), 7381-7399.

[17] S. Khindri; A. Cahn; M. Begg; M. Montembault; C. Leemereise; Y. Cui; A. Hogg; H. Wajdner; S. Yang; J. Robertson; J. N. Hamblin; A. Ludwig-Sengpiel; O. Kornmann; E. M. Hessel, A Multicentre, Randomized, Double-Blind, Placebo-Controlled, Crossover Study To Investigate the Efficacy, Safety, Tolerability, and Pharmacokinetics of Repeat Doses of Inhaled Nemiralisib in

Adults with Persistent, Uncontrolled Asthma. *J Pharmacol Exp Ther* **2018,** *367* (3), 405-413.

[18] E. Hirsch; V. L. Katanaev; C. Garlanda; O. Azzolino; L. Pirola; L. Silengo; S. Sozzani; A. Mantovani; F. Altruda; M. P. Wymann, Central role for G protein-coupled phosphoinositide 3-kinase gamma in inflammation. *Science* **2000,** *287* (5455), 1049-1053.

[19] S. M. Horwitz; R. Koch; P. Porcu; Y. Oki; A. Moskowitz; M. Perez; P. Myskowski; A. Officer; J. D. Jaffe; S. N. Morrow; K. Allen; M. Douglas; H. Stern; J. Sweeney; P. Kelly; V. Kelly; J. C. Aster; D. Weaver; F. M. Foss; D. M. Weinstock, Activity of the PI3K-delta,gamma inhibitor duvelisib in a phase 1 trial and preclinical models of T-cell lymphoma. *Blood* **2018,** *131* (8), 888-898.

[20] S. Dong; B. K. Harrington; E. Y. Hu; J. T. Greene; A. M. Lehman; M. Tran; R. L. Wasmuth; M. Long; N. Muthusamy; J. R. Brown; A. J. Johnson; J. C. Byrd, PI3K p110delta inactivation antagonizes chronic lymphocytic leukemia and reverses T cell immune suppression. *J Clin Invest* **2019,** *129* (1), 122-136.

[21] M. M. Kaneda; K. S. Messer; N. Ralainirina; H. Li; C. J. Leem; S. Gorjestani; G. Woo; A. V. Nguyen; C. C. Figueiredo; P. Foubert; M. C. Schmid; M. Pink; D. G. Winkler; M. Rausch; V. J. Palombella; J. Kutok; K. McGovern; K. A. Frazer; X. Wu; M. Karin; R. Sasik; E. E. Cohen; J. A. Varner, PI3Kgamma is a molecular switch that controls immune suppression. *Nature* **2016,** *539* (7629), 437-442.

[22] B. Ruffell; L. M. Coussens, Macrophages and therapeutic resistance in cancer. *Cancer Cell* **2015,** *27* (4), 462-472.

[23] O. De Henau; M. Rausch; D. Winkler; L. F. Campesato; C. Liu; D. H. Cymerman; S. Budhu; A. Ghosh; M. Pink; J. Tchaicha; M. Douglas; T. Tibbitts; S. Sharma; J. Proctor; N. Kosmider; K. White; H. Stern; J. Soglia; J. Adams; V. J. Palombella; K. McGovern; J. L. Kutok; J. D. Wolchok; T. Merghoub, Overcoming resistance to checkpoint blockade therapy by targeting PI3Kgamma in myeloid cells. *Nature* **2016,** *539* (7629), 443-447.

[24] J. Adams, Targeting PI3K-δ and PI3K-γ in hematological malignancies with duvelisib (IPI-145). [abstract]. In: Proceedings of the AACR Special Conference: Targeting the PI3K-mTOR Network in Cancer; Sep 14-17, 2014; Philadelphia, PA. Philadelphia (PA): AACR; Mol Cancer Ther 2015;14(7 Suppl):Abstract nr IA19

[25] I. W. Flinn; S. O'Brien; B. Kahl; M. Patel; Y. Oki; F. F. Foss; P. Porcu; J. Jones; J. A. Burger; N.

Jain; V. M. Kelly; K. Allen; M. Douglas; J. Sweeney; P. Kelly; S. Horwitz, Duvelisib, a novel oral dual inhibitor of PI3K-delta,gamma, is clinically active in advanced hematologic malignancies. *Blood* **2018,** *131* (8), 877-887.

[26] S. L. Locatelli; G. Careddu; S. Serio; F. M. Consonni; A. Maeda; S. Viswanadha; S. Vakkalanka; L. Castagna; A. Santoro; P. Allavena; A. Sica; C. Carlo-Stella, Targeting Cancer Cells and Tumor Microenvironment in Preclinical and Clinical Models of Hodgkin Lymphoma Using the Dual PI3Kdelta/gamma Inhibitor RP6530. *Clin Cancer Res* **2019,** *25* (3), 1098-1112.

[27] T. A. Yap; L. Bjerke; P. A. Clarke; P. Workman, Drugging PI3K in cancer: refining targets and therapeutic strategies. *Curr Opin Pharmacol* **2015,** *23*, 98-107.

[28] A. E. Garces; M. J. Stocks, Class 1 PI3K Clinical Candidates and Recent Inhibitor Design Strategies: A Medicinal Chemistry Perspective. *J Med Chem* **2019,** *62* (10), 4815-4850.

[29] A. Berndt; S. Miller; O. Williams; D. D. Le; B. T. Houseman; J. I. Pacold; F. Gorrec; W. C. Hon; Y. Liu; C. Rommel; P. Gaillard; T. Ruckle; M. K. Schwarz; K. M. Shokat; J. P. Shaw; R. L. Williams, The p110 delta structure: mechanisms for selectivity and potency of new PI(3)K inhibitors. *Nat Chem Biol* **2010,** *6* (2), 117-124.

[30] J. R. Somoza; D. Koditek; A. G. Villasenor; N. Novikov; M. H. Wong; A. Liclican; W. Xing; L. Lagpacan; R. Wang; B. E. Schultz; G. A. Papalia; D. Samuel; L. Lad; M. E. McGrath, Structural, biochemical, and biophysical characterization of idelalisib binding to phosphoinositide 3-kinase delta. *J Biol Chem* **2015,** *290* (13), 8439-8446.

[31] J. A. Burkhard; B. Wagner; H. Fischer; F. Schuler; K. Muller; E. M. Carreira, Synthesis of azaspirocycles and their evaluation in drug discovery. *Angew Chem Int Ed Engl* **2010,** *49* (20), 3524-3527.

[32] E. M. Carreira; T. C. Fessard, Four-membered ring-containing spirocycles: synthetic strategies and opportunities. *Chem Rev* **2014,** *114* (16), 8257-8322.

[33] Z. Fang; Y. Song; P. Zhan; Q. Zhang; X. Liu, Conformational restriction: an effective tactic in 'follow-on'-based drug discovery. *Future Med Chem* **2014,** *6* (8), 885-901.

[34] Y. J. Zheng; C. M. Tice, The utilization of spirocyclic scaffolds in novel drug discovery. *Expert Opin Drug Discov* **2016,** *11* (9), 831-834.

[35] X. Ma; J. Wei; C. Wang; D. Gu; Y. Hu; R. Sheng, Design, synthesis and biological evaluation of novel benzothiadiazine derivatives as potent PI3Kdelta-selective inhibitors for treating

B-cell-mediated malignancies. *Eur J Med Chem* **2019,** *170*, 112-125.

Highlights

- Structurally novel PI3Kδ/γ dual inhibitors were discovered via the incorporation of a seven-membered spirocyclic building block as the spacer.
- SARs study identified compound **26** as the most potent one throughout this series.
- Compound **26** remarkably attenuated the PI3K signaling in SU-DHL-6 cells.
- Compound **26** displayed a favorable oral bioavailability of 87.5% in SD rats.

Declaration of interests

✔ The authors declare that they have no known competing financial interests or personal relationships that could have appeared to influence the work reported in this paper.

☒The authors declare the following financial interests/personal relationships which may be considered as potential competing interests: